Ultrasonic Pulse Velocity Testing for Monitoring the Degradation of Infill Masonry Walls and Access Their Impact on the Durability of the Envelope of Buildings with Reinforced Concrete Structure

JOSÉ MIRANDA DIAS
Department of Buildings,
National Laboratory of Civil Engineering (LNEC),
Av. do Brasil 101, Lisboa,
PORTUGAL

Abstract: - Buildings with reinforced concrete structure (RCS buildings), including unreinforced masonry (URM) infill walls, can be negatively affected by anomalies in their envelope, such as cracking and water penetration, which worsen the aesthetic aspect and reduce the safety and level of comfort of those buildings. To access the relevance of these anomalies and their evolution along service life, a corresponding survey and monitoring during service life are essential. Non-destructive test methods (NDT), in particular ultrasonic pulse velocity (UPV) testing, are currently used in that survey and monitoring. In the context of monitoring the degradation of the URM infill walls and access their impact on the durability of the RCS building envelope, UPV testing can be a type of NDT method to be used, considering that it can contribute to the evaluation of the state of conservation of the construction elements, such as masonry and concrete.

It is intended here to access the potential use of UPV testing in the monitoring of anomalies related to the degradation of building facades due, particularly, to cracking and to water penetration associated with WDR (wind driven-rain). The preliminary assessment of the use of UPV testing is made through the previous analysis of the results of the application of UPV testing for the detection of sub-surface and surface cracking in compression tests of masonry specimens. Following that analysis, an evaluation is made of the conditioning aspects of the use of UPV testing to access durability problems of the building envelope. Particularly, the main characteristics of cracking with interest for the assessment of the potential use of UPV testing are generally discussed. And, finally, an evaluation is made of the risk of water penetration through the cracks, for potential use of UPV testing in monitoring the presence of humidity in the cracks.

Key-Words: Ultrasonic pulse velocity testing; Infill masonry walls; Buildings; Service life; Durability

Received: April 15, 2023. Revised: July 7, 2023. Accepted: September 4, 2023. Published: September 21, 2023.

1 Introduction

Buildings with reinforced concrete structure (RCS buildings), including unreinforced masonry (URM) infill walls, can be negatively affected by anomalies in their envelope, such as cracking and water penetration, which worsen the aesthetic aspect and reduce the safety and level of comfort of those buildings. To access the relevance of these anomalies and their evolution along service life, a corresponding survey and monitoring during service life are essential. Non-destructive test methods (NDT), in particular ultrasonic pulse velocity (UPV) testing, are currently used in that survey and monitoring, especially in the case of heritage buildings, which can be justifiable, due to their cultural/historical importance and public utility, to use these methods. In the context of monitoring the degradation of the URM infill walls and access their impact on the durability of the RCS building envelope, UPV testing can be a type of NDT method to be used, considering that it can contribute to the evaluation of the state of conservation of the construction elements, such as masonry and concrete. The use of UPV testing for monitoring building envelope, along their service life, could be based on the determination of the rate of spread of ultrasonic waves through their construction elements (particularly, URM infill walls and RCS elements), for a possible estimation of the respective compactness and stiffness.

It is intended here to access the potential use of UPV testing in the monitoring of anomalies related to the degradation of building facades due, particularly, to cracking and to water penetration associated with WDR (wind-driven rain). The preliminary assessment of the use of UPV testing is made through the previous analysis of the results of

the application of UPV testing for the detection of sub-surface and surface cracking in compression tests of masonry specimens. Following that analysis, an evaluation is made of the conditioning aspects of the use of UPV testing to access durability problems of the building envelope. Particularly, the main characteristics of cracking with interest for the assessment of the potential use of UPV testing for their monitoring are generally discussed. Finally, an evaluation is made of the risk of water penetration through the cracks, for potential use of UPV testing in monitoring the presence of humidity in the cracks.

2 Need for Improved Knowledge about the Use of UPV Testing for Monitoring the Degradation of URM Infill Walls and the Methodology of the Present Study

The durability of the RCS building envelope can be significantly affected by degradation agents related to the current external environmental conditions, [1], mainly associated with normal actions of temperature, rain, wind, air pollutants, and biological action, as well as related to climate changes, [2], [3]. The potential use of UPV testing in the monitoring of anomalies of the RCS building envelope should deal with the assessment of the impact of those degradation agents in that envelope. Their common adverse impact on the RCS building envelope is particularly related to the degradation of the facades, which mainly are due to the cracking and detachment of renders and paintings of the URM infill walls and to water penetration through that cracking, associated with WDR (wind-driven rain), as well as the deterioration of externally exposed concrete elements. Water penetration in buildings can decrease their internal conditions of health and comfort.

Cracking of masonry walls of building envelope can occur due to diverse causes, which one of the more relevant are related to deformations of URM infill walls and confining structural elements due to temperature and moisture variations and to vertical loads of the structural elements that support the walls, [1], [4].

Masonry is a composite material made with bricks and mortar adjusted in many different bonding. Usually, the wall section can be correspondent to a single leaf or two leaves of different thicknesses, which can be connected or separated by an internal layer, filled with insulation material, or not filled at all (void space). The knowledge of characteristics of the URM infill walls and the respective technique of construction is essential to analyze the anomalies that occur in the RCS building envelope, but, sometimes, these characteristics are not fully known. The use of non-destructive testing techniques (NDT), such as ultrasonic pulse velocity (UPV) testing, has been used currently in the survey of anomalies to obtain a better knowledge of the constitution of the URM infill walls and to investigate more profoundly their anomalies, considering that different causes of cracking are possible, [5]. UPV testing could attempt to be used for capturing the signs of degradation of the envelope along service life, particularly of relevant sub-surface and superficial cracking that can occur mainly associated with any of these referred causes.

Therefore, UPV testing can be an option for monitoring the degradation and durability of infill masonry walls, but there is a need to improve the knowledge about the conditions of their use, particularly to access the advantages and disadvantages of the use of UPV testing for monitoring the anomalies in facades related to their cracking.

The main motivation behind this work is to study more deeply the characteristics of cracking as well as the assessment of the risk of water penetration through the cracks, for the assessment of the potential use of UPV testing for monitoring the cracking and the presence of humidity in the cracks.

Taking into account the referred need for improved knowledge on the application of UPV testing in RCS buildings, the methodology of the present study will consist of the evaluation of the potential use of UPV testing in monitoring the degradation and accessing the durability of URM infill walls of RCS building envelope. The referred degradation is due, particularly, to cracking and water penetration associated with WDR (wind-driven rain), including climate change effects on buildings. That assessment will be made through the previous analysis of the results of the application of UPV testing for the detection of sub-surface and surface cracking in compression tests of masonry specimens. Following that analysis, an evaluation will be made of the conditioning aspects of the use of UPV testing to access the durability problems of the building envelope. The main characteristics of cracking with interest for the assessment of the potential use of UPV testing for their monitoring are generally discussed. Finally, the evaluation of the risk of water penetration through the cracks, for

potential use of UPV testing in monitoring the presence of humidity in the cracks will be made.

3 Basic Characteristics of UPV Testing and Their Ability for Monitoring the Degradation of Construction Elements as Infill Masonry Walls and Concrete Elements

The ultrasonic pulse velocity (UPV) testing consists of the analysis of the relation between the velocity of elastic waves that propagate in a solid medium and the properties of that medium. For the specific case of construction materials, such as concrete and masonry, higher frequency waves are used in the ultrasonic range (20 kHz to 150 kHz). The device more commonly used consist on a central module, which emits waves, and two transducers (an emitter of pulses of ultrasonic longitudinal waves and a receiver), being the central module to processes the reading and recording of the transmission time. Other type of device, specifically used to obtain improved measuring accuracy, is the ultrasound tomography, where a multi-head antenna equipped with many independent ultrasonic transducers induces the elastic waves.

The use of UPV testing in the mechanical characterization of materials, such as masonry and concrete, is based on the assumption of a relation between the parameters of propagation of ultrasonic waves and the elastic properties of these materials, [6], [7], [8], [9]. Particularly, the wave speed was found dependent on the elastic properties of the transmitting medium, its density and Poisson's ratio, [7].

Concerning the use of UPV testing for the identification of deterioration in materials, some of the parameters that characterize the elastic waves, such as wave speed, generally, are influenced by the existence of damage in the materials, [10]. The propagation velocities of longitudinal waves generally decrease for a damaged material and, particularly, the amplitude of these waves and the speed of propagation of ultrasound are significantly influenced by the presence of surface and subsurface cracks in the material.

The heterogeneity of the material or large voids result in rapid wave attenuation and eventual restriction of the waves from passing through the material, [9]. Flaws, voids, and other type of similar defects increase the transit time of the ultrasonic pulses, [11]. Applied to buildings, these characteristics of UPV testing can help in monitoring the degradation of construction elements, especially due to their sub-cracking and surface cracking. However, the results of UPV testing can be affected by minor defects of the surface or their roughness, due to the restriction, from passing voids, of the short wavelength of the signal, between the surface and the receiver, even in case of minor voids. That leads to the importance of a careful study of the interaction between subsurface cracks and wave parameters. This NDT method has been currently employed to determine the strength of concrete and masonry, to detect voids and discontinuities in the concrete structure, and to test crack depths. Combined with this use of ultrasound testing, thermography and photogrammetry has been used for detection of surface and internal cracks, [5].

UPV testing can be used, particularly, for the primary assessment of the masonry constituent's material's condition, in order to take the adequate intervention, [12]. NDT can be especially helpful in finding hidden features, such as internal voids and flaws and characteristics of the wall section, which cannot be known otherwise than through destructive tests, [5], [12]. UPV testing can be also considered a potential NDT for the detection of significant variations in the moisture content of masonry wall constituents and their rendering, [1].

4 Laboratory Tests

UPV tests were made on masonry specimens subjected to axial compression, aiming to assess, in a laboratory-controlled setting, the advantages and limitations of their use for detection of sub-surface and surface cracking in URM infill of buildings, [5]. Two specimens were tested: Specimen A1 made of vertically perforated ceramic blocks (Figure 1); Specimen A2 made of massive concrete blocks of expanded clay aggregates (Figure 2). These two masonry specimens were subjected to axial compression, until they reached a state of significant cracking, but without reaching a global collapse. Due to the different dimensions of Specimen A1 and Specimen A2, the tests were made in two different compression press machines, which were, for each of the specimens, considered more suitable (Figure 3, Figure 4, Figure 6 and Figure 8).

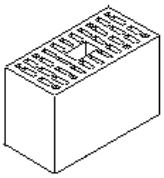
a) Schematic view of the block


b) Top view of the block

Fig. 1: Type of vertically perforated ceramic blocks used in the Specimen A1 (compression test of the specimen)

During the test of both specimens, for each loading step, after reaching the corresponded maximum load level, the specimen was discharged. Immediately after that discharge, the horizontal and vertical deformations were measured with alongameter (registering, after unloading, the deformations in the face A of the specimen – Figure 5 and Figure 7). Horizontal deformations measurements, were made in the upper course of the specimen (dh1 (A1-A2), dh2 (A3-A4)) and in the lower course of the specimen (dh3 (A5-A6), dh4 (A7-A8)).

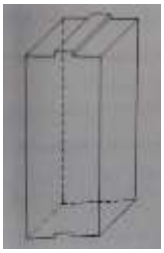
a) Schematic view of the block


b) Partial lateral view of the block

Fig. 2: Type of massive concrete blocks of expanded clay aggregates used in the Specimen A2 (compression test of the specimen)


a) Specimen A1 (perforated ceramic blocks)


b) Specimen A2 (massive concrete blocks of expanded clay aggregates)

Fig. 3: General view of compression test of masonry specimens (view of the face A of the specimens)


a) Specimen A1 (perforated ceramic blocks)


b) Specimen A2 (massive concrete blocks of expanded clay aggregates)

Fig. 4: UPV testing in the compression test of Specimen A1 and Specimen A2

Vertical deformations measurements, were made between the upper and lower course, in the left part of the specimen (dv1 (A1-A5), dv2 (A2-A6) and in the right part of the specimen (dv3 (A3-A7), dv4 (A4-A8). In addition, the vertical absolute displacement of central point D1 in Face B of the two specimens was measured for check control of the specimen tests.

In addition, the ultrasound velocity measurements (direct and indirect measurements; for distance of 100 mm; 200 mm, 300 mm and 400 mm) were made during these tests breaks (3 readings for the measurements in each distance). Then, after the conclusion of the UPV measurements, a new phase load was initiated.

During the loading phase of the specimens, UPV testing was used in the tests for the evaluation of their ability for detection of initial sub-surface cracking in the masonry specimens, and of the evolution of that cracking during the referred axial compression test. Particularly, it was evaluated the degree of sensitivity of UPV testing to detect, with the progressive increment of applied vertical load, the increased opening of the cracks in the masonry.

5 Description of the Test Setup of the Specimens

In the following the description of the test setup of the Specimen A1 and Specimen A2 is made.

5.1 Description of the Test Setup of Specimen A1

Specimen A1 (Figure 3a) was built with vertically perforated ceramic blocks (Figure 1), with two courses of bricks linked between them thorough cement mortar joints (bed joints) as well as the vertical joints. The average dimensions of the blocks were, approximately, 296 mm (length) x 137 mm (thickness) x 193 mm (height). The average percentage of voids of the blocks was approximately

51%. The value of the compressive strength of blocks was near 21.4 N/mm^2. The average dimensions of Specimen A1 were approximately, 600 mm (length) x 137 mm (thickness) x 415 mm (height).

During the test of Specimen A1, a gradual axial compression load was applied, with loading steps of 50 kN (applied vertical stress of 1.23 MPa), 100 kN (2.47 MPa), 200 kN (4.93MPa), 300 kN (7.40 MPa), 400 kN (9.86 MPa)), and final load of 470 kN (11.59 MPa); then ended this loading phase.

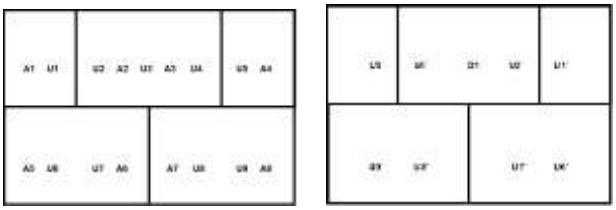

Face A Face B

Fig. 5: Schematic representation of the frame points for horizontal and vertical deformations measurements (points A1 to A8) in face A, and ultrasound measurements in face A and Face B of Specimen A1 in the compression test

Face A Face B

Fig. 6: The phase of preparation of Specimen A1 for the compression test (view of the face A and B of the specimen)

5.2 Description of the Test Setup of Specimen A2

Specimen A2 (Figure 3b) was built with massive concrete blocks of expanded clay aggregates (Figure 2b), with four courses of blocks linked thorough cement mortar joints (bed joints) as well as the vertical joints. The average dimensions of the blocks were approximately 490 mm (length) x 145 mm (thickness) x 190 mm (height). The value of the compressive strength of blocks was near 10.1 N/mm^2. The average dimensions of Specimen A1 were, approximately, 750 mm (length) x 145 mm (thickness) x 810 mm (height).

In the loading phase of Specimen A2, a gradual axial compression load was applied, with loading steps of 50 kN (applied vertical stress of 0.54 MPa), 100 kN (1.07 MPa), 200 kN (2.15 MPa), 300 kN (3.22 MPa), 400 kN (4.30 MPa), and final load of 490 kN (13.98 MPa); then ended this loading phase.

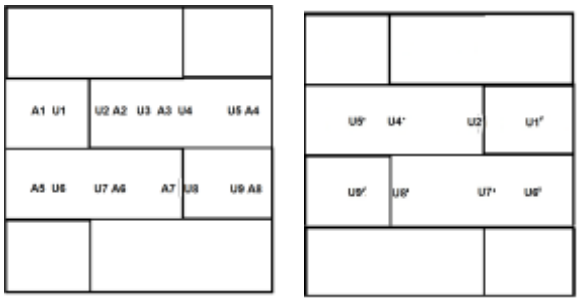

Face A Face B

Fig. 7: Schematic representation of the frame points for horizontal and vertical deformations measurements (points A1 to A8) in face A, and for ultrasound measurements in face A and face B of Specimen A2 in the compression test

Face A Face B

Fig. 8: Phase of preparation of Specimen A2 for the compression test (view of specimen face A and B)

6 Results of the Tests

The results of the compression test of both specimens (Specimen A1 and Specimen A2), in terms of the measurement of horizontal and vertical deformations with alongameter, and of the UPV tests, are following presented.

6.1 Test Results of Specimen A1

The results of the measurement of vertical deformations (dv1 to dv4) and horizontal deformations (dh1 to dh4), in the face A of the specimen, for each loading step after the discharge of the specimen, are presented in Table 1 (vertical deformations) and Table 2 (horizontal deformations). The results of UPV tests on Specimen A1 are presented in Tables 3 (indirect method), Table 4 (direct method), Table 5 (Appendix) and Table 6 (Appendix). During the test, with the increasing of the load, the specimen was gradually showing signs of surface cracking, and fragmentation (Figure 9). At the end the specimen was extensively damaged (Figure 10, Figure 11, Figure 12, Figure 13 and

Figure 14), especially in the left part of face A of the specimen (Figure 10 and Figure 11), with fragmentation of the top of corner zone. The right part of face B of the specimen (Figure 12 , Figure 13 and Figure 14) was also severely damaged, with fragmentation of almost the entire corner zone of the specimen and with a near vertical crack of the of the upper brick near the referred corner zone.

Table 1. Vertical deformations in the test of Specimen A1

Load (kN)	**Vertical deformations**							
	A1 - A5	ε_{Vm}	A2 - A6	ε_{Vm}	A3 - A7	ε_{Vm}	A4 - A8	ε_{Vm}
/(MPa)	dv1	mm/m	dv2	mm/m	dv3	mm/m	dv4	mm/m
0/0	942	0	1069	0	1110	0	818	0
50/1.23	947	-0.025	1070	-0.005	1115	-0.025	819	-0.005
100/2.47	945	-0.015	1067	0.01	1111	-0.005	818	0
200/4.93	949	-0.035	1073	-0.02	1115	-0.025	817	0.005
300/7.40	951	-0.045	1074	-0.025	1124	-0.07	819	-0.005
400/9.86	950	-0.04	1084	-0.075	1148	-0.19	823	-0.025

Unity=0.001 mm; Base of measurement = 200 mm

Table 2. Horizontal deformations in the test of Specimen A1

Load (kN)	**Horizontal deformations**							
	A1-A2	ε_{Hm}	A3-A4	ε_{Hm}	A5-A6	ε_{Hm}	A7-A8	ε_{Hm}
/(MPa)	dh1	mm/m	dh2	mm/m	dh3	mm/m	dh4	mm/m
0/0	940	0	981	0	960	0	852	0
50/1.23	932	0.04	980	0.005	955	0.025	853	-0.0025
100/2.47	926	0.07	978	0.015	957	0.015	855	-0.0075
200/4.93	918	0.11	960	0.105	955	0.025	851	0.0025
300/7.40	892	0.24	890	0.455	955	0.025	820	0.08
400/9.86	870	0.35	842	0.695	954	0.03	788	0.16

After reaching the maximum load of 470 kN (Applied vertical stress of 11.59 MPa), with the collapse of the specimen (Figure 9, Figure 10, Figure 11 and Figure 12), the test was halted and the specimen was discharged.

Fig. 9: Aspect of the face A of the Specimen A1 in the compression test, with signs of local fragmentation of the top part of specimen (left side of the specimen)

Fig. 10: Aspect of the face A of Specimen A1 at the end of the test after discharge of a load of 470 kN

Fig. 11: Aspect of the face A of Specimen A1 at the end of the test with the collapse of the specimen

Fig. 12: Aspect of the face B of Specimen A1 at the end of the test

Fig. 13: Aspect of the face B of Specimen A1 at the end of the test

Fig. 14: Aspect of the face B of Specimen A1 at the end of the test

Table 3. Results of ultrasound test of specimen A1 by indirect method for zero load (0 kN - 3 readings for each measurement between two points)

Method		Indirect method Time (microseconds)						
		U1-U2	U1-U3	U1-U4	U1-U5	U6-U7	U6-U8	U6-U9
Distance		100	200	300	400	100	300	400
Readi	1	95.1	199.4	306.2	313.1	78.9	418	506.2
	2	95.1	199.4	305.5	314.1	79.5	357.6	509.2
	3	95.1	199.4	306.6	314.5	79.7	418.3	574.9
Mean		95.1	199.4	306.1	313.9	79.4	398.0	530.1

Table 4. Results of ultrasound test of specimen A1 by direct method for zero load (0 kN - 3 readings for each measurement between two points)

Method		Direct method Time (microseconds)							
		U1-U1	U2-U2	U4-U4	U5-U5	U6-U6	U7-U7	U8-U8	U9-U9
Distance		150	150	150	150	150	150	150	150
Readings	1	95	87,8	84,8	89,1	87,3	87,3	82,2	82,7
	2	95	87,4	84,6	88,8	87,3	87,8	82,9	82,7
	3	95,1	87,4	84,6	89,1	87,3	87,3	82,9	83
Mean		95,0	87,5	84,7	89,0	87,3	87,5	82,7	82,8

6.2 Test Results of Specimen A2

The results of the measurement of vertical deformations (dv1 to dv4) and horizontal deformations (dh1 to dh4) with alongameter in the face A of the specimen, for each loading step after the discharge of the specimen, are presented in Table 7 (vertical deformations) and Table 8 (horizontal deformations). The results of UPV tests on Specimen A2 are presented in Table 9, Table 10, Table 11 (Appendix) and Table 12 (Appendix).

During the test, with the increasing load, the specimen was gradually showing signs of slight surface cracking in mortar joints (Figure 13, Appendix) and, at the end of the test, signs of local fragmentation of the base of the face B of Specimen A2 were evident.

After reaching the maximum load of 490 kN (Applied vertical stress of 5.26 MPa), with the slight cracking and local fragmentation of the base of the face B of the specimen (Figure 15, Figure 16, and Figure 17), the test was halted and the specimen was discharged.

Table 7. Vertical deformations in the test of Specimen A2

Load (kN)	Vertical deformations							
	A1-A5	ε_{Vm}	A2-A6	ε_{Vm}	A3-A7	ε_{Vm}	A4-A8	ε_{Vm}
/(MPa)	dv1	mm/m	dv2	mm/m	dv3	mm/m	dv4	mm/m
0/0	913	0	945	0	851	0	778	0
50/0.54	925	-0.06	980	-0.18	882	-0.16	788	-0.05
100/1.07	942	-0.15	1010	-0.33	900	-0.25	794	-0.08
200/2.15	944	-0.16	1063	-0.59	935	-0.42	798	-0.1
300/3.22	986	-0.37	1093	-0.74	959	-0.54	802	-0.12

400/4.30	1004	-0.46	1130	-0.93	1000	-0.75	821	-0.22
490/5.26	918	-0.03	936	0.05	848	0.02	778	0

Unity=0.001 mm; Base of measurement = 200 mm

Table 8. Horizontal deformations in the test of Specimen A2

Load (kN)	Horizontal deformations							
	A1-A2	ε_{Hm}	A3-A4	ε_{Hm}	A5-A6	ε_{Hm}	A7-A8	ε_{Hm}
/(MPa)	dh1	mm/m	dh2	mm/m	dh3	mm/m	dh4	mm/m
0/0	957	0	970	0	1010	0	970	0
50/0.54	942	0.08	965	0.03	1009	0.01	967	0.02
100/1.07	924	0.17	964	0.03	997	0.07	967	0.02
200/2.15	432	2.63	964	0.03	492	2.59	982	-0.06
300/3.22	175	3.91	954	0.08	190	4.1	994	-0.12
400/4.30	128	4.15	933	0.19	140	4.35	987	-0.09
490/5.26	297	3.3	525	2.23	250	3.8	530	2.2

Unity=0.001 mm; Base of measurement = 200 mm

Fig. 15: Aspect of the Specimen A2 in the compression test, with signs of slight surface cracking in mortar joints

Fig. 16: Aspect of the face A of Specimen A2 at the end of the test

Fig. 17: Aspect of the face B of Specimen A2 at the end of the test, with evident signs of local fragmentation of the base of specimen

Table 9. Results of ultrasound test of Specimen A2 by indirect method for zero load (0 kN - 3 readings for each measurement between two points)

Method		**Indirect method Time (microseconds)**						
		U1-U2	U1-U3	U1-U4	U1-U5	U6-U7	U6-U8	U6-U9
Distance		100	200	300	400	100	300	400
Readings	1	93,1	182,9	236,2	291,8	47,4	143,7	221,9
	2	92,9	182,7	237,6	291,5	46,6	143,2	221,3
	3	91,8	182,4	238,3	293,1	47,5	143,7	221,5
Mean		92,6	182,7	237,4	292,1	47,2	143,5	221,6

Table 10. Results of ultrasound test of Specimen A2 by direct method for zero load (0 kN - 3 readings for each measurement between two points)

Method		**Direct method Time (microseconds)**							
		U1-U1	U2-U2	U4-U4	U5-U5	U6-U6	U7-U7	U8-U8	U9-U9
Distance		150	150	150	150	150	150	150	150
Readings	1	58,5	58,5	57,8	59,1	59,9	60,3	60,8	60,4
	2	58,5	57,7	57,8	58,6	59,9	60,0	60,6	60,4
	3	59,3	57,7	58,5	58,6	59,9	60,2	61,1	60,4
Mean		58,8	58,0	58,0	58,8	59,9	60,2	60,8	60,4

7 Analysis of Test Results of Specimen A1

The results of the Specimen A1, related to the measurement of horizontal and vertical deformations with alongameter (Figure 18 and Figure 19) and UPV testing are analyzed in the following, to access the potential use of UPV testing in the detection of sub-surface cracking in the corresponding type of masonry walls. The analysis of the results of the Specimen A1 test is carried out in the following, according to their relevant phases, and particularly with emphasis on the results of UPV testing. Three phases of the test are considered: load between 0 kN and 100 kN (2.47 MPa); load between 100 kN and 300 kN (7.40 MPa); and load between 300 kN (7.40 MPa) and the final load of 470 kN (11.59 MPa).

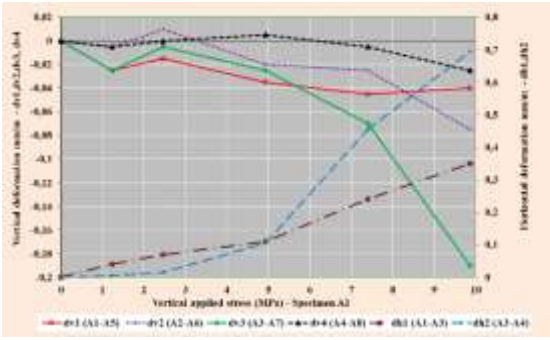

Fig. 18: Results of deformations measurements in the compression test of Specimen A1, for increasing levels of vertical applied stress - vertical deformations (dv1, dv2, dv3, dv4) in the left vertical axis; horizontal deformations (dh1, dh2) in the right vertical axis

The results of the measurement of deformations in Specimen A1 show that, after the initial phase of the test (initial phase between 0 and 50 kN) until a load of near 300 kN, the overall variation of horizontal and vertical deformations corresponded, respectively, to a gradual horizontal expansion and vertical contraction of the specimen. These measured deformations are presented in Figure 18 and Figure 19. These variations of the vertical and horizontal measured deformations during the test of Specimen A1 are relevant to help in the analysis of the UPV testing results, and their detailed analysis is developed in the following sub-chapters 7.1 to 7.3.

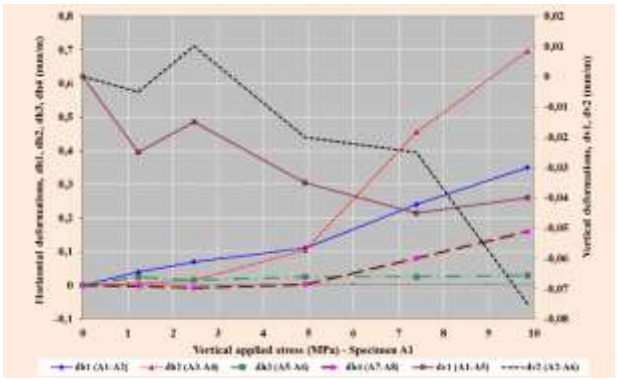

Fig. 19: Results of deformations measurements in the compression test of Specimen A1, for increasing levels of vertical applied stress - horizontal deformations (dh1, dh2, dh3, dh4) in the left vertical axis; vertical deformations (dv1, dv2) in the right vertical axis

7.1 Range of Load between 0 kN and 100 kN (2.47MPa)

In this phase of load between load zero and 100 kN (2.47MPa), the vertical and horizontal deformations did not reveal an appreciable change of values (Figure 18 and Figure 19), and no significant signs of visible surface cracking were detected. The variation of the vertical deformations (dv1, dv2, dv3, and dv4), in the test of Specimen A1, show an initial phase of slight contraction of the specimen, from load zero to 50 kN (1.23 MPa), with increasing negative moderate values (Figure 18). That was followed by a vertical expansion, from 50 kN (1.23 MPa) to 100 kN (2.47 MPa), with a reduction of the negative values (expansion) and a positive value being reached for 100 kN of load (Figure 18), in the particular case of dv2 measurement (left side of face A, in the upper course of bricks).

For this range of load between load zero and 100 kN, horizontal deformations in the upper course, dh1 and dh2 (Figure 19), show increasing positive values (expansion), since the start of the test. In the lower course, dh3 (A5-A6: right side of face A) only show increasing positive values until a 50 kN of load, after which it reduced the positive value (contraction). For a load of 50 kN and 100 kN, dh4 registered a constant positive low value (expansion), since the start of the test until a 50 kN of load (Figure 19).

The application of UPV testing in this phase of the test of Specimen A1 reveals an acceptable correlation between mean time and the distance of measurement in the upper course, U1 to U5 (mean time of U1-U2, U1-U3, U1-U4, U1-U5), for the readings made in the start of the test. These

readings were made after the discharge of 0 kN of load (Figure 20a); the first load step of 50 kN (Figure 20b); and the load step of 100 kN (Figure 20c). The correspondent correlation for the lower course was also acceptable with the exception of the meantime of U6 to U9 related to the readings made in the first load step of 50 kN (Figure 18b) due to the significant deviation of U6-U7 reading (distance of 300 mm – reading that include the central vertical joint – Figure 5). In the horizontal deformations measurements h3 and h4, which were made in the zone common to the U6-U7 reading (lower course), it was detected, at 50 kN of load, a contraction that also constitutes some type of deviation face to the others zones that were in expansion.

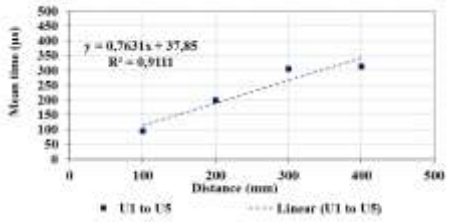

a) U1-U5: Applied vertical load = 0 kN

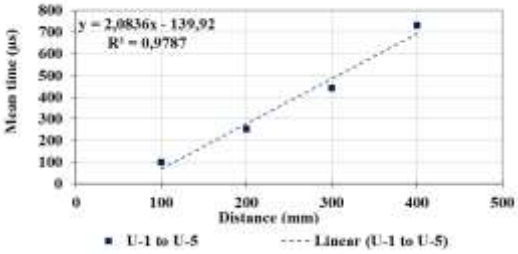

b) U1-U5: Applied vertical load = 50 kN (1.23 MPa)

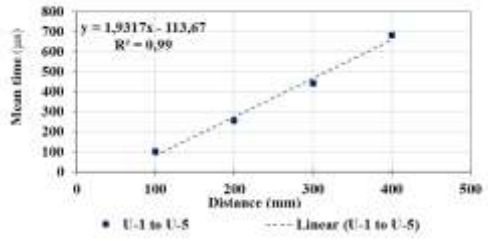

c) U1-U5: Applied vertical load = 100 kN (2.47 MPa)

Fig. 20: Correlation between mean time and distance of measurement in UPV testing (indirect method: U1-U2 (distance of 100 mm); U1-U3 (200 mm); U1-U4 (300 mm); and U1-U5 (400 mm)), for levels of 0 kN, 50 kN and 100 kN of vertical applied stress in the compression test of Specimen A1

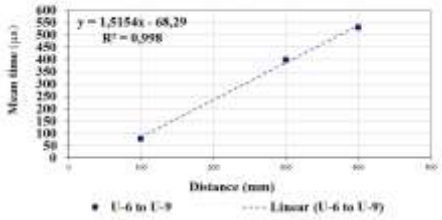

a) U6-U9 - Applied vertical load = 0 kN

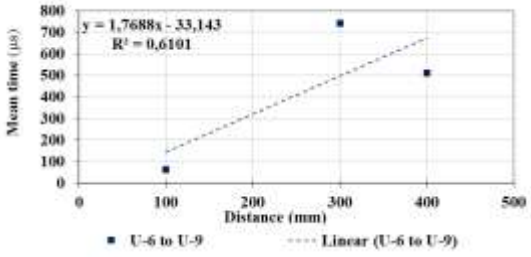

b) U6-U9 - Applied vertical load = 50 kN (1.23 MPa)

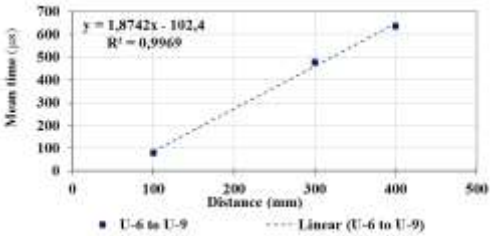

c) U6-U9 - Applied vertical load = 100 kN (2.47 MPa)

Fig. 21: Correlation between mean time and distance of measurement in UPV testing (indirect method: U6-U7 (distance of 100 mm); U6-U8 (300 mm); and U6-U9 (400 mm)), for levels of 0 kN, 50 kN and 100 kN of vertical applied stress in the compression test of Specimen A1

Concerning the UPV testing, in this phase of test, with the application of the first load step of 50 kN (1.23 MPa), the ultrasound velocity (direct method), registered a slight change in relation to that registered for 0 kN of load (Figure 21, Figure 22, Figure 23, Figure 24 and Figure 25). A decrease in U1-U1, U4-U4, U5-U5, U7-U7 and U8-U8 readings and an increase in U2-U2, U6-U6, and U9-U9

readings was registered. That type of slight change, with no dominant trend in variation of the ultrasound velocity, is considered not relevant in this initial phase of load, where the effects of accommodation of the specimen to the initial load could be relevant. In the subsequent step load of 100 kN (2.47 MPa), there was a slight decrease of ultrasound velocity in all readings, which could indicate that the effects of vertical expansion occurred between these two steps of load (50 kN-100 kN) did not change significantly the wave transmission across the thickness of the specimen.

The ultrasound velocity in the direct method, in this phase of load, had light decrease of values for 50 kN and 100 kN in relation to the value for 0 kN, indicating a minor change of the internal material structure of the specimen. In respect of values of the calculated ultrasound velocity in the face A (indirect method), with the application of the first load step of 50 kN (1.23 MPa), there was an appreciable decrease of the ultrasound velocity measured after discharge of that load, relatively to the correspondent value for 0 kN. That decrease was registered for all the readings, except for U6-U7 (as referred before this zone was in contraction, in opposite to other zones of the specimen that were in expansion) and U6-U9 readings. During this range of load between 0 kN and 100 kN, no signs of surface cracking were detected in the specimen.

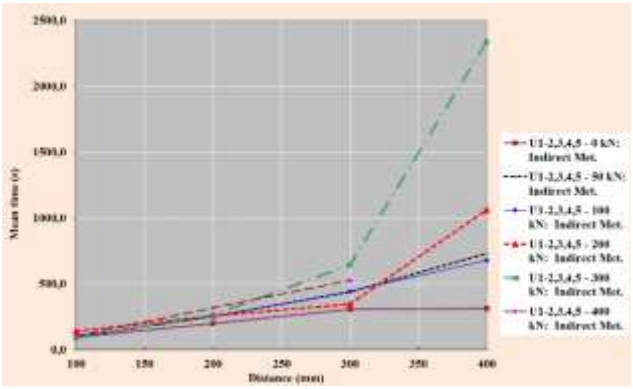

Fig. 22: Results of UPV testing in the compression test of Specimen A1, in terms of Meantime/Distance of measurement (Indirect method, Mean time of 4 readings U1- U2 (100 mm); U1-U3 (200 mm); U1-U4 (300 mm); U1-U5 (400 mm))

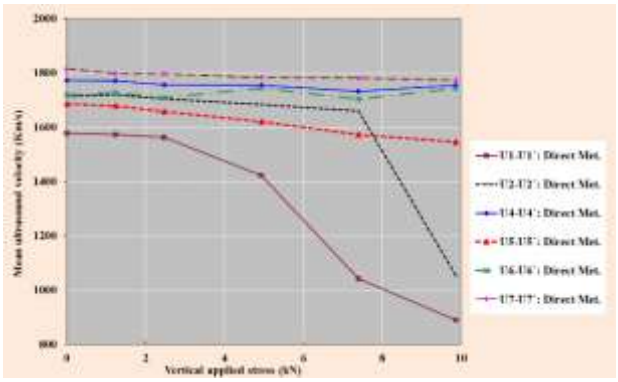

Fig. 23: Ultrasound velocity (direct method) for increasing levels of vertical applied stress in the compression test of Specimen A1

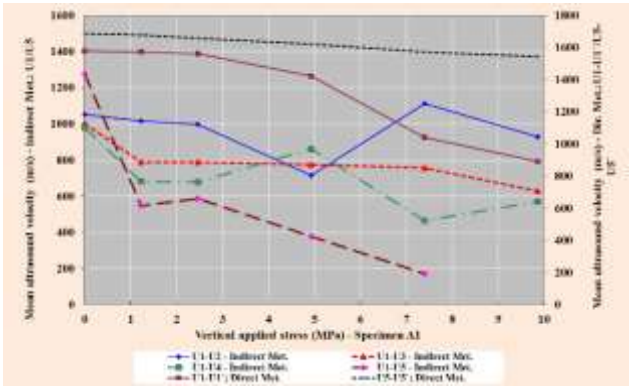

Fig. 24: Ultrasound velocity (indirect method: U1/U5 and direct method: U1-U1, U5-U5) in the compression test of Specimen A1

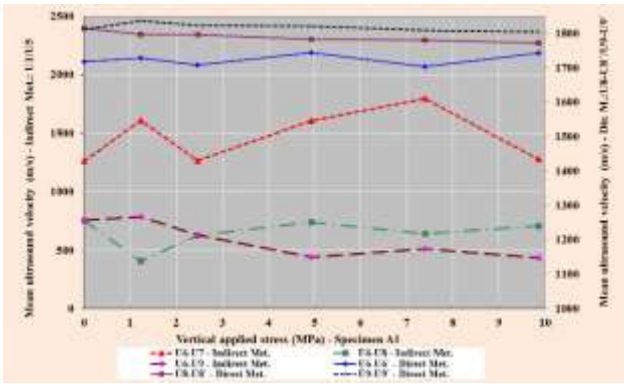

Fig. 25: Mean ultrasound velocity (indirect method: U6/U9 and direct method: U6-U6, U8-U8 U9-U9) in the compression test of Specimen A1

7.2 Range of Load between 100 kN (2.47 MPa) and 300 kN (7.40 MPa)

After discharge of a load level of 200 kN (4.93 MPa), the registered vertical deformations dv1, dv2 and dv3 show negative values associated to contraction (for load 100 kN (2.47 MPa), these deformations values were positive), while dv4 increased their positive value (expansion). Between the levels of load of 200 kN (4.93 MPa) and of 300 kN (7.40 MPa), vertical deformations dv1, dv2 and dv3 follow the increase of negative values (contraction), especially deformation dv3 which show a stronger increase, meanwhile vertical deformation dv4 reduced their positive value (contraction) and reached a negative value (Figure 18).

For this range of load between 100 kN and 300 kN, horizontal deformations in the upper and lower course, (Figure 19), show increase positive values (expansion), although especially moderate in case of lower course when compared with that of upper course, which suggests that micro sub-surface cracking in the face A of the Specimen was growing. That micro sub-surface cracking could be spreading in the face A, especially in the upper course, although still not very relevant and not clearly visible.

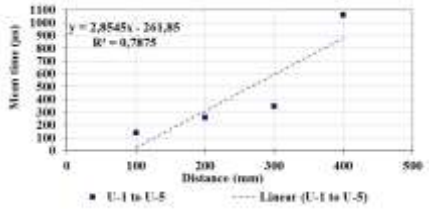

a) U1-U5: Applied vertical load = 200 kN

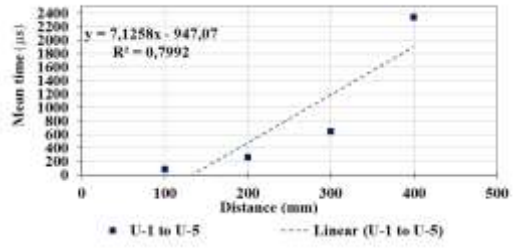

b) U1-U5: Applied vertical load = 300 kN

Fig. 26: Correlation between mean time and distance of measurement in UPV testing (indirect method: U1-U2 (distance of 100 mm); U1-U3 (200 mm); U1-U4 (300 mm); and U1-U5 (400 mm)), for levels of 200 kN and 300 kN of vertical applied stress in the compression test of Specimen A1

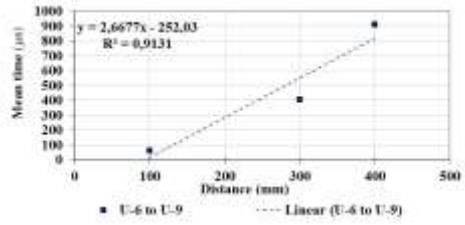

a) U6-U9 - Applied vertical load = 200 kN

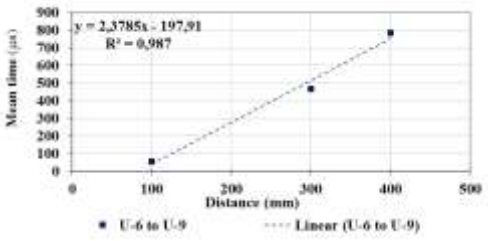

b) U6-U9 - Applied vertical load = 300 kN

Fig. 27: Correlation between mean time and distance of measurement in UPV testing (indirect method: U6-U7 (distance of 100 mm); U6-U8 (300 mm); and U6-U9 (400 mm)), for levels of 200 kN and 300 kN of vertical applied stress in the compression test of Specimen A1

About the UPV testing, in this phase of the test of Specimen A1, the correlation between mean time and the distance of measurement in the upper course, U1 to U5, was not as straight as in the previous phase (Figure 10). That correlation refers to the mean time of U1-U2, U1-U3, U1-U4, and U1-U5: correlation for 200 kN and 300 kN, respectively in Figure 26a and Figure 26b. That could be due to alterations of surface integrity related to early micro sub-surface cracking in the face A of specimen A1. That agrees with the above indication, revealed by horizontal deformations measurements in the upper course, of a micro sub-surface cracking upsurge in this phase of load.

The correspondent correlation for the lower course (U6 to U9) was better than that obtained for upper course, either for 200 kN and for 300 kN (respectively in Figure 27a and Figure 27b). That corroborates with the results of the moderate horizontal deformations measurements h3 and h4, in this loading phase, which were made in the zone common to the U6-U9 reading.

The values of ultrasound velocity (direct method), in this phase of load of the Specimen A1 test, generally, decreased relatively to the previous values. The exception is the U6-U6′ reading (for 200 kN had an increase followed by a decrease for 300 kN; and U7-U7′ (for 200 kN the value of 100 kN of load maintained, followed by an increase for 300 kN). That increase was notorious, especially after 200 kN, which is a sign that substantial change of the internal material structure of the specimen was in course in this phase of load, above 200 kN.

In respect of values of mean ultrasound velocity in the face A (indirect method), the readings for the load of 200 kN, with the exception of U1-U4 reading, registered a considerable decrease in relation to the previous readings (for 100 kN of load). That could be associated to a substantial change in the surface integrity related to early micro sub-surface cracking in face A.

7.3 Range of Load between 300 kN (7.40 MPa) and Final Load of 470 kN (11.59 MPa)

Between the level of load of 300 kN (7.40 MPa) and of 400 kN (9.86 MPa), the registered vertical deformations, dv2, dv3 and dv4, show increasing negative values associated to contraction (especially dv4, which show a stronger increase - Figure 18), while dv1 reduced their negative value (expansion). Horizontal deformations in the upper and lower course, in this phase of load (Figure 19), follow the increase of positive values (expansion) of the previous phase, particularly accentuated in case of upper course when compared with that of lower course (dh3 had a moderate increase). That could indicate a significant process of sub-surface cracking of the bricks in the face A of the Specimen, especially of their upper part. That part of the specimen, at the end of the test, showed more signs of extensive surface cracking (Figure 11, Figure 12, Figure 13 and Figure 14), mainly in the left upper part of face A (and right upper part of Face B).

In the US measurements of Specimen A1 test, for 400 kN of load, the correlation between mean time and the distance of measurement, in the upper course, was solely correspondent to the readings from U1 to U4 (mean time of U1-U2, U1-U3, U1-U4: correlation in Figure 28). That was due the difficulty of obtaining the U1-U5 reading, which restricted the full application, in the left and central part of Face A, of the US readings. Although limited to U1 to U4, that correlation can be considered satisfactory. The correspondent correlation for the lower course was possible from U6 to U9, but was not as fair as the previous one (Figure 29), which could be in correspondence with the results of the moderate horizontal deformations measurements h3 (common zone to the U6-U9 reading), when compared to the h4 measurement.

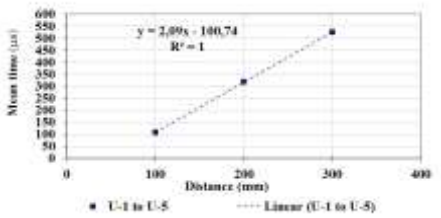

a) U1-U5: Applied vertical load = 400 kN

Fig. 28: Correlation between mean time and distance of measurement in UPV testing (indirect method: U1-U2 (distance of 100 mm); U1-U3 (200 mm); U1-U4 (300 mm); and U1-U5 (400 mm)), for levels of 400 kN of vertical applied stress in the compression test of Specimen A1

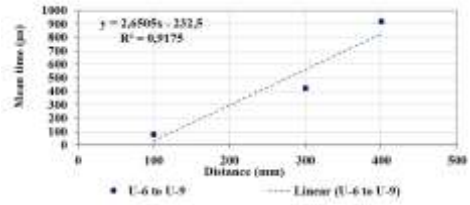

a) U6-U9 - Applied vertical load = 400 kN

Fig. 29: Correlation between mean time and distance of measurement in UPV testing (indirect method: U6-U7 (distance of 100 mm); U6-U8 (300 mm); and U6-U9 (400 mm)), for levels of 400 kN of vertical applied stress in the compression test of Specimen A1

The values of ultrasound velocity (direct method), in this phase of load of the Specimen A1 test generally decreased, with the exception of U4-U4′ and U6-U6′. That increase was particularly relevant for U1-U1′ and U2-U2′, which is a sign that extensive surface cracking of the upper left part of the face A of the Specimen was in course which was evident at the end of the test (Figure 10 and Figure 11).

The values of mean ultrasound velocity in the face A (indirect method), namely the reading from U1 to U5, for the load of 400 kN, showed a considerable decrease in relation to the previous reading (for 300 kN of load). The exception was U1-U4 and U6-U8 readings, which had an increase of mean US velocity. That agrees with the findings of the direct method, that extensive surface cracking of the specimen was in course, especially in the upper left part of the face A of the Specimen. At the end of the test, the situation of extensive surface cracking of the upper left part of face A of Specimen A1 was fully revealed (Figure 11).

8 Analysis of Test Results of Specimen A2

The results of the Specimen A2, related to the measurement of horizontal and vertical deformations with alongameter and ultrasound tests are analyzed in the following, according to their relevant phases, particularly with emphasis on the results of UPV testing, aiming the access of their potential use in the detection of sub-surface and surface cracking. Three phases of the test, similarly as made for specimen A1, were here considered: load between 0 kN and 100 kN (1.07 MPa); load between 100 kN (1.07 MPa) and 300 kN (3.22 MPa); and load between 300 kN (3.22 MPa) and the final load of 490 kN (5.26 MPa). The results of the measurement of vertical deformations in Specimen A2 show that, during the test, until a load of near 400 kN (4.30 MPa), the overall variation corresponded to a gradual vertical contraction of the specimen.

These vertical and horizontal measured deformations during the test of the specimen A2 are presented in the Figure 30 and Figure 31, and are relevant to help in the analysis of the UPV testing results. Their detailed analysis is developed in the following sub-chapters 8.1 to 8.3.

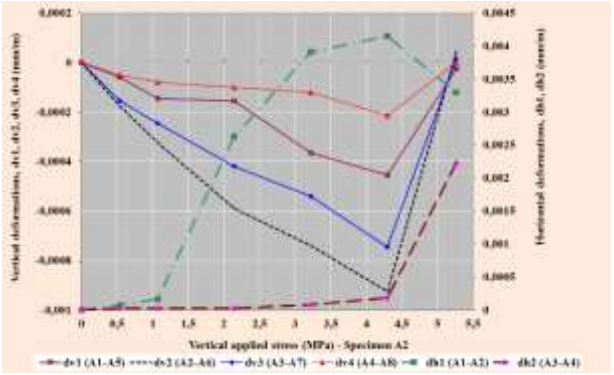

Fig. 30: Results of deformations measurements in the compression test of Specimen A2, for increasing levels of vertical applied stress - vertical deformations (dv1, dv2, dv3, dv4) in the left vertical axis; horizontal deformations (dh1, dh2) in the right vertical axis

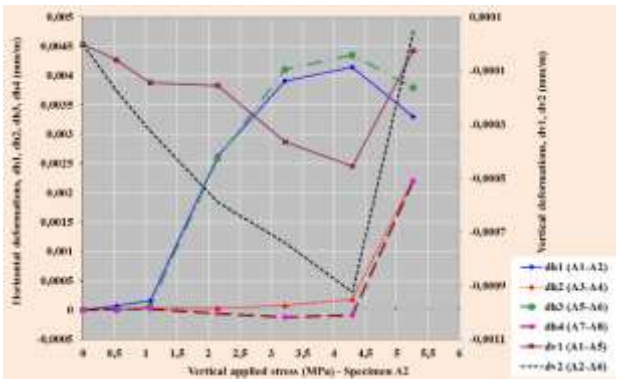

Fig. 31: Results of deformations measurements in the compression test of Specimen A2, for increasing levels of vertical applied stress - horizontal deformations (dh1, dh2, dh3, dh4) in the left vertical axis; vertical deformations (dv1, dv2) in the right vertical axis

8.1 Range of Load between 0 kN and 100 kN (1.07 MPa)

For a load level of 100 kN (1.07 MPa), the registered vertical deformations dv1, dv2, dv3, and dv4 show negative values associated with contraction (Figure 30). For this range of load between load zero and 100 kN, horizontal deformation in the upper course, dh1, and the lower course, dh3 (Figure 31), show increasing positive values (expansion), since the start of the test.

The UPV testing results in this phase of the test of Specimen A2 reveal an acceptable correlation between mean time and the distance of measurement in the upper course, U1 to U5, for the readings made before the start of the test (0 kN of load - Figure 32a); in first load step of 50 kN (Figure 32b); and the load step of 100 kN (Figure 32c), indicating a constant decrease of ultrasound velocity. The correspondent correlation for the lower course, U6 to U9, was also acceptable (Figure 33). With respect to the results of UPV testing in this phase of the load until the step load of 100 kN (1.07 MPa), there was not a clear tendency for the evolution of ultrasound velocity in the readings of the direct method and indirect method (Figure 34, Figure 35, Figure 36 and Figure 37).

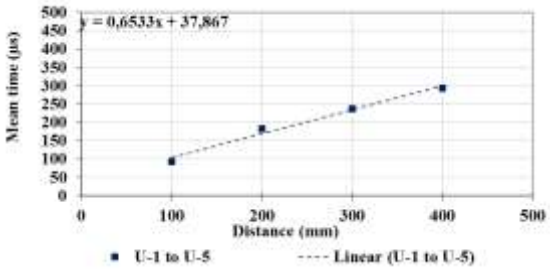

a) U1-U5: Applied vertical load = 0 kN

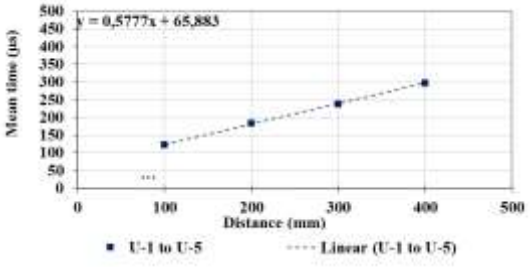

b) U1-U5: Applied vertical load = 50 kN (1.23 MPa)

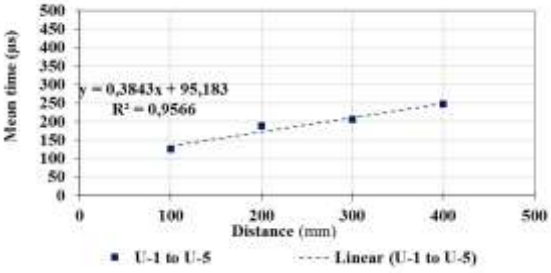

c) U1-U5: Applied vertical load = 100 kN (2.47 -MPa)

Fig. 32: Correlation between mean time and distance of measurement in UPV testing (indirect method: U1-U2 (distance of 100 mm); U1-U3 (200 mm); U1-U4 (300 mm); and U1-U5 (400 mm)), for levels of 0 kN, 50 kN and 100 kN of vertical applied stress in the compression test of Specimen A2

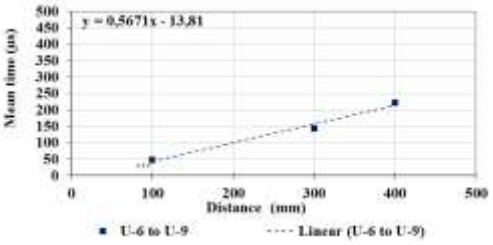

a) U6-U9 - Applied vertical load = 0 kN

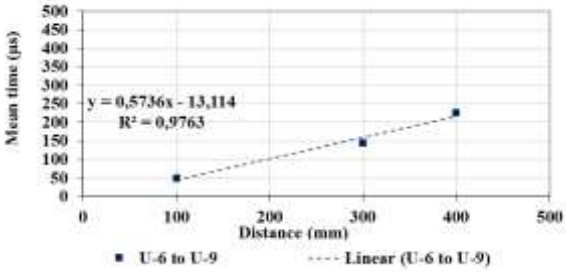

b) U6-U9 - Applied vertical load = 50 kN (1.23 MPa)

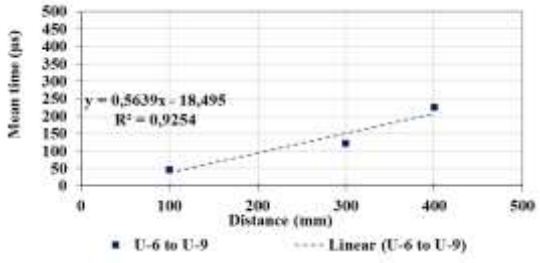

c) U6-U9 - Applied vertical load = 100 kN (2.47 MPa)

Fig. 33: Correlation between mean time and distance of measurement in UPV testing (indirect method: U6-U7 (distance of 100 mm); U6-U8 (300 mm); and U6-U9 (400 mm)), for levels of 0 kN, 50 kN and 100 kN of vertical applied stress in the compression test of Specimen A2

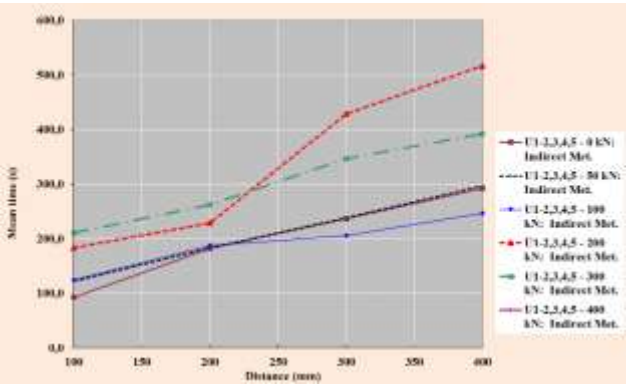

Fig. 34: Results of UPV testing in the compression test of Specimen A2, in terms of Mean time/Distance of measurement (Indirect method, Mean time of 4 readings U1- U2 (100 mm); U1-U3 (200 mm); U1-U4 (300 mm); U1-U5 (400 mm)

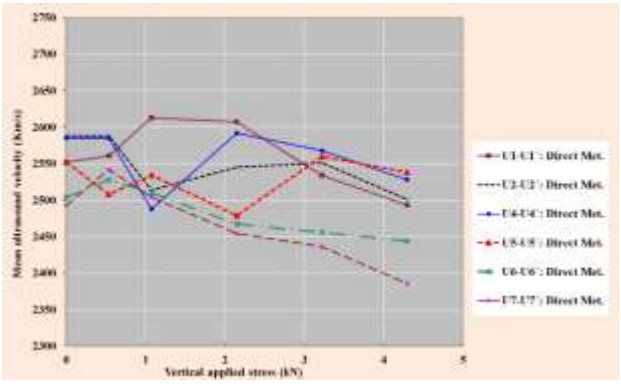

Fig. 35: Ultrasound velocity (direct method) for increasing levels of vertical applied stress in the compression test of Specimen A2

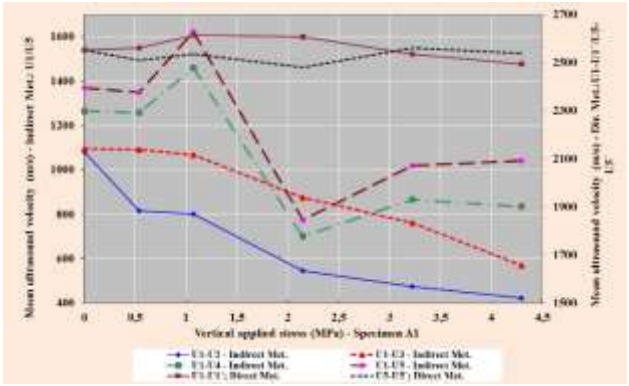

Fig. 36: Ultrasound velocity (indirect method: U1/U5 and direct method: U1-U1, U5-U5) in the compression test of Specimen A2

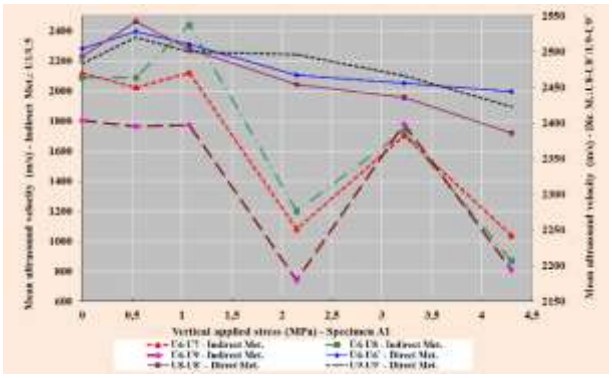

Fig. 37: Mean ultrasound velocity (indirect method: U6/U9 and direct method: U6-U6, U8-U8 U9-U9) in the compression test of Specimen A2

8.2 Range of Load between 100 kN (1.07 MPa) and 300 kN (3.22 MPa)

Between the levels of the load of 100 kN (1.07 MPa) and of 300 kN (3.22 MPa), vertical deformations dv1, dv2, and dv3 follow the increase of negative values (contraction). The horizontal deformations in the upper course, dh1, and lower course, dh3, (Figure 30 and Figure 31), show a constant increase of positive values (expansion), which suggests that micro sub-surface cracking in the face A (left part) of the Specimen A2 was growing in this phase of the test.

The UPV testing results in this phase of the test of Specimen A2 reveal fair correlation between mean time and the distance of measurement in the upper course, U1 to U5, for the readings made in the load step of 200 kN (Figure 38a) and load step of 300 kN (Figure 38b), indicating a constant decrease of ultrasound velocity. The correspondent correlation for the lower course, U6 to U9, was not so fair (Figure 39) indicating that some alterations in the integrity of the specimen were occurring. The values of ultrasound velocity (direct method and indirect method), in this phase of load of the Specimen A2 test, generally, decreased relatively to the previous values (Figure 34, Figure 35, Figure 36 and Figure 37) presumably indicating the onset and progression of sub-surface cracking of the specimen.

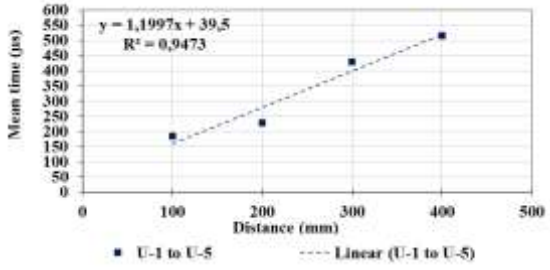

a) U1-U5: Applied vertical load = 200 kN

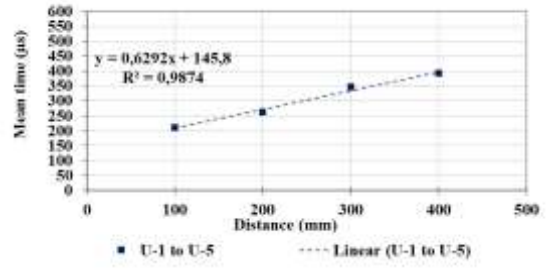

b) U1-U5: Applied vertical load = 300 kN

Fig. 38: Correlation between mean time and distance of measurement in UPV testing (indirect method: U1-U2 (distance of 100 mm); U1-U3 (200 mm); U1-U4 (300 mm); and U1-U5 (400 mm)), for levels of 200 kN and 300 kN of vertical applied stress in the compression test of Specimen A2

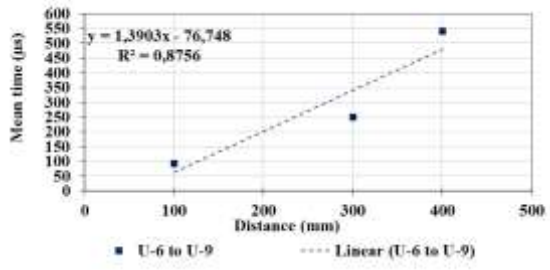

a) -U6-U9 - Applied vertical load = 200 kN

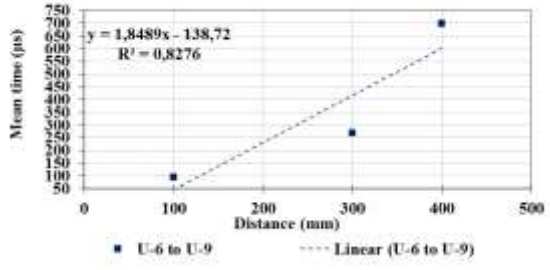

b) U6-U9 - Applied vertical load = 300 kN

Fig. 39: Correlation between mean time and distance of measurement in UPV testing (indirect method: U6-U7 (distance of 100 mm); U6-U8 (300 mm); and U6-U9 (400 mm)), for levels of 200 kN and 300 kN of vertical applied stress in the compression test of Specimen A2

8.3 Range of Load between 300 kN (3.22 MPa) and Final Load of 470 kN (5.26 MPa)

Between the level of load of 300 kN (3.22 MPa) and final load of 470 kN (5.26 MPa), the registered vertical deformations, dv1, dv2, dv3 and dv4 (Figure 30), progress their contraction till the load level of 400 kN (4.30 MPa), after which decreasing negative values were recorded, associated probably to sub-surface cracking of the blocks and mortar joints in face A. Horizontal deformations in the upper and lower course, in this phase of load, follow the increase of positive values (expansion) of the previous phase till the load of 400 kN (Figure 31), after which changed and reduced the positive values, indicating possibly a process of slight sub-surface cracking of the blocks and mortar joints in the face A of the Specimen 2.

In the US measurements of Specimen A1 test, for 400 kN of load, the correlation between mean time and the distance of measurement, in the upper course, was correspondent to the readings from U1 to U5 (mean time of U1-U2, U1-U3, U1-U4, U1-U5: correlation in Figure 40), which can be considered satisfactory. The correspondent correlation for the lower course, from U6 to U9 (Figure 41), can be also considered satisfactory. Concerning of values of mean ultrasound velocity in the face A (direct method and indirect method), the readings for the load of 470 kN, generally, registered a decrease in relation to the previous readings which could be associated to slight cracking of blocks and mortar joints of the face A.

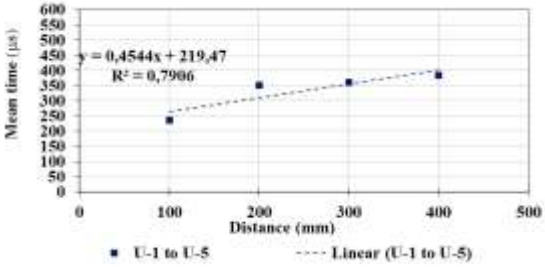

a) U1-U5: Applied vertical load = 400 kN

Fig. 40: Correlation between mean time and

distance of measurement in UPV testing (indirect method: U1-U2 (distance of 100 mm); U1-U3 (200 mm); U1-U4 (300 mm); and U1-U5 (400 mm)), for levels of 400 kN of vertical applied stress in the compression test of Specimen A2

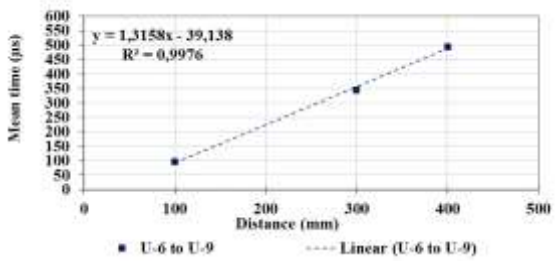

a) U6-U9 - Applied vertical load = 400 kN

Fig. 41: Correlation between mean time and distance of measurement in UPV testing (indirect method: U6-U7 (distance of 100 mm); U6-U8 (300 mm); and U6-U9 (400 mm)), for levels of 400 kN of vertical applied stress in the compression test of Specimen A2

9 Global Analyses of the Results of the Tests of Specimen A1 and of Specimen A2

Based on the results of the measurement of deformations with alongameter and the results of the UPV testing, in compression tests of Specimen A1 and Specimen A2, it can be inferred a general tendency, with the increase of loading in these tests, to a gradual horizontal expansion (an increase of positive values) and vertical contraction (an increase of negative values) of the specimens (Figure 42 and Figure 43) and a reduction of ultrasound velocity (direct and indirect measurements). An almost constant decrease of the values of the ultrasound velocity (indirect measurements (U1-U2), and direct measurement (U1-U1´)) appears to follow that variation trend of horizontal/vertical deformation measurements, for increasing levels of load (Figure 42 and Figure 43).

As an example of this trend, the results of the tests of Specimens A1 and A2 reveal an almost constant increase of the values of horizontal measurements (dh1 and dh3), in the left part of Face A (Figure 42 and Figure 43), of specimens, between the level of load of 50 kN (1.23 MPa (A1) and 0.54 MPa (A2)) and 300 kN (7.40 MPa (A1) and 3.22 MPa (A2)), which generally are higher (in absolute values) than the vertical measurements (more expansion in horizontal direction than contraction in vertical direction, at the left side of face A of the specimens). The values of dh1 (path with one vertical mortar joint, in the upper part of the left side of face A of both specimens) are higher or approximately equal, relative to the dh3 values (path with no mortar joint), which suggests that the influence of the presence of vertical mortar joint is appreciable in the deformation behavior of the specimen, and that distinctive behavior was also reflected in the variation of ultrasound velocity. Ultrasound velocity of the indirect measurements U1-U2, in that upper part, is generally lower than the indirect measurements U6-U7, in the correspondent inferior part, and, probably, that could be related to the decrease of the propagation velocities of longitudinal waves, in case of presence of a mortar joint linking the material of the masonry units (bricks (A1) or blocks (A2)), and the amplitude of these waves and the speed of propagation of ultrasound could be significantly influenced by the discontinuity / in-homogeneity represented by the mortar joint.

Moreover, the presence of vertical mortar joints can change the local pattern of stress and lead to the up-surge of micro cracking in the mortar joints and masonry units. The measured horizontal deformations, for increasing load levels, revealed that could be sensible (more than the measured vertical deformations) to the onset and progression of cracking phenomena observed during the test of the specimens, which corresponded in the same loading steps, to significant alterations of values of ultrasound velocity in the UPV testing. It appears that the behavior revealed by horizontal measurements, for load levels above 200 kN, when the cracking is intensified significantly in both tests of the specimens, could also be reflected in the UPV testing. Therefore, the alterations of the ultrasound velocity in the UPV testing on Specimen A1 and A2 can allow the presumption that, with indirect and direct measurement of the ultrasound velocity, it can be possible the detection of the onset and progression of the micro sub-surface cracking.

In conclusion, the critical discussion made in this section regarding the results tabulated in the previous sections appears to make it fully understandable that the main intention here is to claim and highlight that, with the measurement of ultrasound velocity in the masonry specimens, it could be possible the detection of the onset and progression of the micro sub-surface cracking

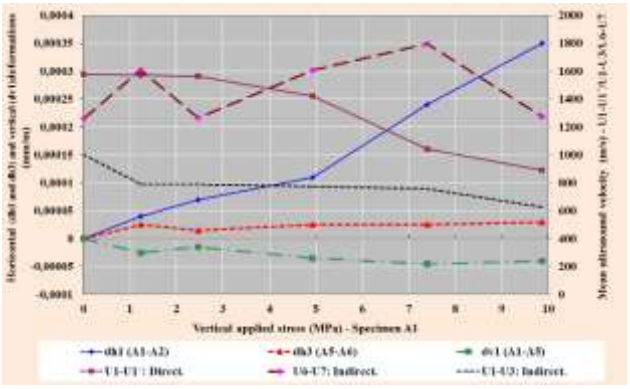

Fig. 42: Results of deformations measurements in the compression test of Specimen A1, for increasing levels of vertical applied stress - horizontal (dh1, dh3) and vertical (dv1) deformations in the left vertical axis; Mean ultrasound velocity (indirect method: U1/U3, U6-U7 and direct method: U1-U1) in the right vertical axis

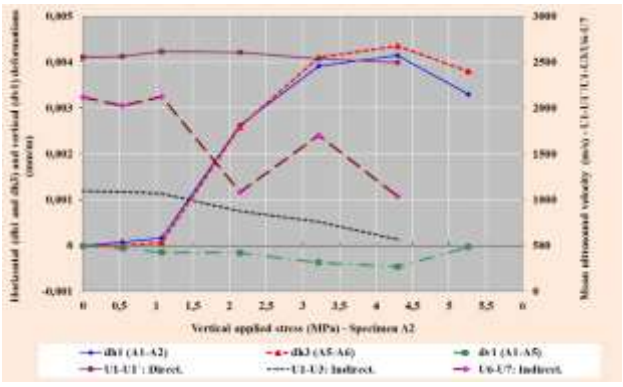

Fig. 43: Results of deformations measurements in the compression test of Specimen A2, for increasing levels of vertical applied stress - horizontal (dh1, dh2) and vertical (dv1) deformations in the left vertical axis; Mean ultrasound velocity (indirect method: U1/U3, U6-U7and direct method: U1-U1) in the right vertical axis

10 Conditioning Aspects of the Use of UPV Testing to Access Durability Problems of Building Envelope Considering the type of Masonry Cracking and Climate Factors

URM infill walls of envelope of RCS buildings are usually subjected to aggressive actions, especially due to the climate factors, which can lead to appreciable degradation of these URM infill walls. That can lead, particularly, to the reduction of durability of the building envelope, associated especially to their degradation, in result of cracking and associated surface erosion of URM infill walls, as well as, water penetration in these walls due to wind-driven rain (WDR), particularly across that cracking. Furthermore, that cracking and associated water penetration, subsequently, can severely worsen their weathering characteristics due, particularly to water infiltration/humidity inside the building, and may lead to considerable weakening of the structural building elements, as their deterioration progress, especially, due to wetting.

Therefore, in the scope, of preventive and/or corrective actions along the service life of the buildings, it is important the monitoring of the durability anomalies, particularly related to cracking of URM infill walls of the envelope of buildings, which can occur along their service life, especially in the case of heritage buildings. As revealed in the previous sections (section 4 to 9), UPV testing could possibly help in the evaluation of the state of conservation of URM infill walls especially in the detection of sub-surface cracks in these walls. UPV testing can possibly be used, besides monitoring of the cracks before an intervention of repair of previous cracking in the envelope, also for a type of monitoring, along building service life, the durability problems in the URM infill walls, particularly related to their cracking and water penetration thorough that cracking. In order to use UPV testing in detection and monitoring of cracks, as well as in the access of the risk of water penetration thorough that cracking, it could be useful to classify the main typologies of cracking to be analyzed by UPV testing, as well as the relevant conditions of exposure to WDR of building envelope.

10.1 Main Characteristics of Cracking with Interest for the Assessment of the Potential Use of UPV Testing for Their Detection and Monitoring

Cracking is a common defect that occurs in facade cladding and it is observed that cracking defects are frequently associated with mechanical actions, [13]. Loads applied to the building envelope can lead to deformations that may cause significant stress that

affects, particularly URM infill walls, [1], [4], as well as other confining construction elements and components. The stresses in URM infill walls, which lead to its cracking, can be the result of axial forces (tension or compression) and of applied shear forces. When normal or shear stress values are larger than, respectively, the normal or shear strength of the material, that create the essential conditions for the formation of a crack, here defined as a physical discontinuity on an element or material, [14].

Cracks characterization can be based on its width, orientation, location, or their extension on the facade. For the assessment of potential degradation of the URM infill walls, it is important to define the characteristics of the cracking, which can lead to subsequent detachment and/or local degradation. That assessment can orientate the effort of monitoring anomalies related to cracking, which are essentially related to the following main characteristics: crack orientation; width of the crack; crack time evolution; crack configuration; a group of cracks of the same type; and crack depth.

These main characteristics of cracks are presented in Table 13 (Appendix), for the assessment of the interest of potential use of UPV testing for their detection and monitoring. In Table 13 (Appendix), a possible classification of the cracks, [15], [16], according to their width is presented: Negligible (0-0.1 mm); Thin (0.1 mm – 1 mm); Medium (2 mm – 3 mm); Large (greater than 3mm). In that Table 13 (Appendix), it is suggested the estimated potential interest for the use of UPV for the assessment of the state of conservation of URM infill walls in relation to these main characteristics of the cracking and of other types of anomalies associated to cracking, assuming different levels of interest: Nupv – Null estimated potential interest for the use of UPV testing; Lupv Low estimated potential interest for the use of UPV testing; Mupv – Medium estimated potential interest for the use of UPV testing; Hupv – High estimated potential interest for the use of UPV testing. That estimation involves the estimation of the importance of the type of cracks in the process of decision about the use of UPV testing, aiming at the definition of corrective intervention.

10.2 Assessment of Potential Use of UPV Testing for Monitoring the Presence of Humidity in Walls and for the Evaluation of the Risk of Water Penetration through Their Cracking

As referred above (in section 3), UPV testing is an interesting NDT method that can be explored to access their potential use for detection of significant variations in moisture content of a URM infill wall. For that detection, it is important to identify the conditioning aspects of the use of UPV testing for that purpose, which should be, especially, related to the relevance of water penetration across the existing cracking, and the consequent risk of degradation of the building facade, particularly of their aesthetic aspect and of the infiltration of humidity inside the building. Therefore, it is important to identify the critical aspects the of transfer of moisture within the walls, particularly related to water penetration inside the walls due to rainwater. The mechanisms of transfer of moisture within the walls are very complex and are mainly related to physical processes of absorption, condensation and capillarity in the constituent materials of the walls, which appears to be not easily identified by UPV testing.

Precipitation accompanied by intense wind is the principal agent accountable for the wetting of building envelopes.

Degradation of building vertical envelope due to micro-cracking of sub-surface and surface of URM infill wall (associated for example to temperature and moisture cyclic variations) can lead to a need of a survey of building envelope, with the use of NDT methods, particularly UPV testing, aiming possible maintenance and repair actions. Micro-cracking upsurge (for example associated with excessive thermal strain) at the external surfaces of the URM infill walls and concrete structure elements can modify the permeability of these external surfaces to the rain with a horizontal velocity component given by the wind, which is called wind-driven rain (WDR). The use of UPV testing could be made when these cracks are partially or completely filled with water after a precipitation period (rain) and/or could be made later, after that precipitation period, when the wall is almost dried particularly the cracks, eventually allowing to compare the results of both readings of UPV testing in different periods.

Among the climatic hazards that are more influential on buildings, particularly heritage buildings, wind-driven rain (WDR) is found to be especially detrimental, as it may cause surface erosion and facilitate moisture penetration and bio-deterioration, [17]. Erosion here means the detachment of material from the masonry of the building facade due to the physical impingement of WDR. Water penetration in the building envelope essentially can occur due to significant absorption of precipitation water (l/m^2) by the vertical surface due

to wind-driven rain (WDR). Semi-empirical equations have been proposed in the literature to compute the amount of wind-driven rain (WDR) incident on a wall.

The amount of WDR, for a selected rainy period, could be calculated using a semi-empirical approach of the ISO model, [18], which is based on the physical correlation of WDR, wind speed, and horizontal rain ($R_{wdr} = \alpha . U_{10} . (R_h)^{0.88} . \cos \theta$ - where α is the WDR coefficient, U_{10} is the wind speed measured 10 m above the ground (m/s), R_h is the horizontal rainfall intensity (mm) and θ is the angle between the wind direction and the normal to the building facade; α, is computed as $\alpha = 0.222.C_R.C_T.O.W$ - where C_R and CT are the roughness and topography coefficients, respectively, while O is the obstruction factor and W is the wall factor. C_R is calculated on the basis of height above the ground (z) and the minimum height (z_{min}) parameters).

In another approach the WDR load, I_{WDR} (kg/m^2s), at building facades, can be obtained by multiplying the horizontal rainfall intensity I_h (kg/m^2 s) by a parameter η ($I_{WDR}=I_h \times \eta (\theta, U_{ref}, I_h)$, where η is a function of the angle θ (°) between reference wind direction and orientation of the wall, reference wind speed U_{ref} (m/s) and I_h, all obtained from meteorological data, [19], [20]. That parameter η could be obtained from measurements, empirical relations, or numerical simulations. Moisture presence caused by WDR can negatively affect the durability of building facades due to degradation of surface material, cracking (especially relevant for larger crack width, and interior damage, [17]. And considering some of the variables involved in the computation of WDR, particularly related to geographical localization of the buildings, it could be inferred that the local implantation of the building probably should condition the potential use of UPV testing, being more useful in case of severe environmental conditions that propitiates the formation of cracking, as well as water penetration through that cracking.

In the evaluation of the risk of water penetration across the existing cracking in the envelope of a building, specifically should be assessed the extent of facade area affected by the cracks, the cracking patterns and the maximum width of the cracks.

If there are only very slight cracks in the URM infill wall (crack width less than 0.1 mm), the sheet of constant and uniform runoff water passes through them without penetrating them, and the portion to be absorbed by the walls is foremost due to the capillarity of the constituent materials of the wall. In these cases, the wind associated with the incident rain acts on the wall creating a pressure difference between the wall and the sheet of runoff water, [16]. Thus, this sheet is, by this effect, forced to penetrate the wall; the most significant portion of the water migration to the interior of the wall is then processed through cracks with significant crack width (greater than 0.1 mm), through which the sheet of runoff water passes in its downward trajectory. These cracks are most often located in the area of vertical and horizontal mortar joints. It should be noted that, at the end of the precipitation period (rain), a considerable part of the moisture absorbed by the surface layer of the wall evaporates through a drying process, the speed of which depends on the climatic conditions (temperature, wind, relative humidity of ambient air). In case of elements of the building envelope of solid material such as solid bricks (non-perforated bricks) or concrete, generally the presence of humidity in the very small voids of the solid material, possibly, increases the speed of propagation of ultrasound in relation to the correspondent values of the dry material, considering that the path of longitudinal waves has less alterations that in case of dry material. And, regarding the use of UPV testing for detection of cracks in these solid materials, the presence of humidity in the cracks can lead to misleading results in what concern the detection of these cracks and the estimation of their depth. Therefore, it is important to study more deeply the applicability of UPV testing for the accessing the cracks filled with humidity.

In case of building vertical envelope with absence of defects or pores larger than 1 mm, the pressure difference across the facade (difference of indoor and outdoor wind pressure) is the most sensitive factor related to water penetration, regardless of the existing water supply, [21]. However, in case of building vertical envelope with defects, pores, or larger cracks (>5 mm), water is able to penetrate the facade, even without high wind pressure. For facades with defects, pores, and cracks of less than 1 mm, the influence of wind pressure in water penetration is dominant, while, in the case of damaged or poorly maintained facades, the major influence in the penetration process is the amount of water falling on the facade, [21]. Experimental studies, [16] indicated that, for values of incident water flow (“iwf”) in walls ranging between 100 l/h and 240 l/h, the infiltrated water flow (“fiw”) in walls could tend to be higher in horizontal mortar joints (“hmj”), than in vertical mortar joints (“vmj”). In vertical joints “fiw” could be, likely, lower for a crack width of 0,7 mm, when compared to a crack width of 1 mm to 2 mm, which indicates that UPV

testing should concentrate on monitoring walls with cracks above 1 mm. Besides the referred trend, a general tendency for the increase, with the rise of differential pressure on the wall, of the ratio between the infiltrated water flow and the incident water flow in the wall (assuming a constant value of 240 l/h for "iwf"). And, for the case of "fiw", it could be expected that, for a crack width around 0,7 mm, a reduction of that ratio with increase of "iwf" in walls, regardless of the values of differential pressure acting on wall, also indicating the tendency for a more dominant effect of "iwf" on "fiw", when compared to the effect of differential pressure on "fiw". It could be referred that, as an example, the value of incident water flow ("iwf") and of sob-pressure in the wall could be around respectively, 2,3 l/m^2 and 480 Pa, which approximately could correspond to a value of precipitation of 140 mm/h, accompanied by the wind speed of 100 km/h (27,8 m/s).

The previewed more intense rain and increase in temperatures due to climate changes will accentuate the adversity of present environmental conditions in terms of water penetration through the cracking in the walls. Therefore, it could be of convenience for choosing different intensities (periodicity) of monitoring the cracking in the URM infill walls using UPV testing after an intervention of repair, considering the scenarios correspondent to assessments of projected future changes using Representative Concentration Pathways (RCPs) that can influence durability problems in buildings, [3]. A more intense monitoring could be advised for scenario of high greenhouse gas emission, about RCP 8.5, when compared to the monitoring that can be advised for the scenario of low greenhouse gas emission, Scenario A, about RCP 4.5, being the first scenario (RCP 8.5), less favorable, supposed to lead to predictable greater intensity of rain and higher increase in temperature variations due to climate changes, relatively to that previewed for RCP 4.5 scenario.

Taking into account the previous considerations made in this sub-section, in Table 13 (Appendix), it is suggested the estimated potential interest for the use of UPV testing for monitoring the presence of humidity in walls and for the evaluation of the risk of water penetration through their cracking, in parallel to what was suggested in sub-section 10.1, about the main characteristics of the cracking.

11 Conclusion

An evaluation was here made of the potential use of UPV testing in the monitoring of the degradation of the URM infill walls and access their impact on the durability of the RCS building envelope. The degradation of URM infill walls of building facades due, particularly, to cracking and to water penetration associated to WDR (wind driven rain), including climate change effects, was here especially focused.

That assessment was made through the previous analysis of the results of the application of UPV testing for the detection of sub-surface and surface cracking in compression tests of masonry specimens. Based on the results of the measurement of deformations with alongameter and the results of the UPV testing, in the referred compression tests of Specimen A1 and Specimen A2, it can be inferred a general tendency, with the increase of loading in these tests, to a gradual horizontal expansion (increase of positive values) and vertical contraction (increase of negative values) of the specimens, and a reduction of ultrasound velocity (direct and indirect measurements). An almost constant decrease of the values of the ultrasound velocity (indirect measurements, and direct measurement) appears to follow that variation trend of horizontal/vertical deformation measurements, for increasing levels of load.

The results of the tests of Specimens A1 and A2 reveal that the influence of the presence of vertical mortar joint is appreciable in the deformation behavior of the specimen, and that distinctive behavior was reflected in the variation of ultrasound velocity.

Moreover, the presence of vertical mortar joints can change the local pattern of stress and lead to the up-surge of micro cracking in the mortar joints and masonry units. The measured horizontal deformations, for increasing load levels, revealed that could be sensible (more than the measured vertical deformations) to the onset and progression of cracking phenomena observed during the test of the specimens, which corresponded in the same loading steps, to significant alterations of values of ultrasound velocity in the UPV testing. Therefore, the alterations of the ultrasound velocity in the UPV testing on Specimen A1 and A2 can allow the presumption that, with indirect and direct measurement of the ultrasound velocity, it can be possible the detection of the onset and progression of the micro sub-surface cracking.

Following that analysis of compression tests of masonry specimens, an evaluation was made of the conditioning aspects of the use of UPV testing to access durability problems of the building envelope. The main characteristics of cracking with interest for the assessment of the potential use of UPV

testing for their monitoring were generally discussed. That assessment can orientate the effort of monitoring anomalies related to cracking, which are essentially related to their main characteristics.

Finally, an evaluation was made of the risk of water penetration through the cracks, for potential use of UPV testing in monitoring the presence of humidity in the cracks. Moisture presence caused by WDR can negatively affects the durability of building facades due to degradation of surface material, cracking (especially relevant for larger crack width, interior damage. And considering some of the variables involved in the computation of WDR, particularly related to geographical localisation of the buildings, it could be inferred that the local implantation of the building probably should condition the potential use of UPV testing, being more useful in case of severe environmental conditions that propitiates the formation of cracking, as well as water penetration through that cracking.

Regarding the contributions of this work concerning to previous works in literature, a comprehensive analysis of the characteristics of cracking, as well as the assessment of the risk of water penetration through the cracks is considered to have been suitably made in this paper, with positive repercussions in terms of their better knowledge. That knowledge could be useful, in terms of the practical applicability for the assessment of the potential use of UPV testing for the monitoring of the cracks and water penetration through the cracks.

Thus, it is admitted that the present paper can provide, for future scientific research work, a helpful reference for UPV testing, considering the contribution of the paper in revealing the relation between ultrasound velocity and the upsurge of micro-cracking in masonry.

As possible future developments of this work, it is recommendable that should be further studied, deeply, the benefits and limitations of the use of UPV testing for monitoring the degradation and access the durability of URM infill walls of the RCS building envelope, considering the type of URM infill walls cracking and the climate factors.

References:

[1] Miranda Dias, J. L.; Matias, L.; Henriques, M. J., Deformations and volume changes due to moisture variations in heritage buildings - Use of NDT techniques. 18th International Flow Measurement Conference (Flomeko2019). LNEC,2019. http://repositorio.lnec.pt:8080/jspui/handle/123456789/1011864

[2] Lacasse, M. A.; Gaur, A.; Moore, T. V., Durability and climate change - implications for service life prediction and the maintainability of buildings. Buildings 2020, 10, 53. doi:10.3390/buildings10030053.

[3] Miranda Dias, J. L., Matias, L.; Henriques, M. J., Impact of climate change on the durability of heritage buildings with structural concrete elements and masonry walls. Fib Symposium-Concrete Structures: New Trends for Eco-Efficiency and Performance. Lisboa, 2021. pp. 1971-1981. http://repositorio.lnec.pt:8080/jspui/handle/123456789/1013989

[4] Miranda Dias, J. L., Damage of Infill Masonry Walls due to Vertical Loads in Buildings with Reinforced Concrete Structure. WSEAS Transactions on Applied and Theoretical Mechanics, vol. 18, 2023, pp. 32-49. https://wseas.com/journals/articles.php?id=7765

[5] Miranda Dias J. L., Matias L., Henriques M. J., Ribeiro, M. S. Santos, T. O., Combined use of non-destructive methods for the survey of facades anomalies of heritage buildings with structural concrete elements. 7th International Conference on Engineering Surveying (INGEO2017),LNEC,2017. http://repositorio.lnec.pt:8080/jspui/handle/123456789/1010126

[6] Chung, H. W.; Law, K. S., Diagnosis in situ concrete by ultrasonic pulse technique. Concrete International, 1983.

[7] Liang M.T., Wu, J., Theoretical elucidation on the empirical formulae for the ultrasonic testing method for concrete structures. Cement and Concrete Research, Vol. 32, Issue 11, 2002, pp. 1763-1769. https://doi.org/10.1016/S0008-8846(02)00866-9

[8] Popovics, S., Analysis of the concrete strength versus ultrasonic pulse velocity relationship. The American Society for Non-Destructive Testing (ASNT), 2010.

[9] Schuller, M. P.; R. H. Atkinson and J. L. Noland, "Structural Evaluation of Historic Masonry Buildings," APT Bulletin, vol. 26, no. 2/3, 1995, pp. 51-61.

[10] Naik, T. R; Malhotra, V. M., The ultrasonic pulse velocity method. Handbook on non-destructive testing of concrete. Boca Raton: CRC Press, 1991, pp. 169-88.

[11] Komlos K., Popovics S., Nűrnbergerová T., Babd B., Popovics J. S., Ultrasonic Pulse

Velocity Test of Concrete Properties as Specified in Various Standards. Cement and Concrete Composites, 18, 1996, pp. 357-364.

[12] Binda A. L., Application of NDTs to the diagnosis of Historic Structures. SAISI NDTCE'09, Non-Destructive Testing in Civil Engineering. Nantes, France, 2009.

[13] Pereira C., Silva A., Brito J., Flores-Colen I., Silvestre J., Contribution of Cracking and Spalling to the Degradation of Façade Claddings in Current Buildings. CIB World Building Congress 2019, Hong Kong SAR, 2019

[14] Bonshor, R. B., Bonshor, L. L. 1996. Cracking in Buildings. BRE: Garston, 1996

[15] CIB (International Council for Research and Innovation in Building and Construction), Defects in Masonry Walls. Guidance on Cracking: Identification, Prevention and Repair - Prevention of Cracking in Masonry Walls. W023, Wall Structures. CIB Publication 403, ISBN 978-90-6363-090-4.

[16] Miranda Dias, J. L., Cracking occurring in building external masonry walls associated with rainwater infiltration *(in Portuguese)*. 3º ENCORE Proceedings, LNEC, 2003, pp. 1129-1138. http://repositorio.lnec.pt:8080/jspui/handle/123456789/1002836

[17] Erkal A., D'Ayala D. B. L., Sequeira L., Assessment of wind-driven rain impact, related surface erosion and surface strength reduction of historic building materials. Building and Environment Volume 57, 2012, Pages 336-348 https://doi.org/10.1016/j.buildenv.2012.05.004

[18] European Committee for Standardization, EN ISO 15927-3: Hygrothermal Performance of Buildings - Calculation and Presentation of Climatic Data, Part 3: Calculation of a Driving Rain Index for Vertical Surfaces from Hourly Wind and Rain Data, CEN, Brussels, 2009.

[19] Abuku M., Janssen H., Roels S., Impact of wind-driven rain on historic brick wall buildings in a moderately cold and humid climate: numerical analyses of mould growth risk, indoor climate and energy consumption. Energy Build., 41, 2009, pp. 101-110, https://doi.org/10.1016/j.enbuild.2008.07.011

[20] Blocken, B.; Carmeliet, J., Spatial and temporal distribution of wind-driven rain on low-rise building. Wind and Structure, Volume 5, Number 55, 2002, pp. 441-462. https://doi.org/10.12989/was.2002.5.5.441

[21] Pérez-Bella, J. M.; Domínguez-Hernández, J.; Rodríguez-Soria, B.; Coz-Díaz, J. J.; Cano-Suñén, E., Combined use of wind-driven rain and wind pressure to define water penetration risk into building façades: The Spanish case. Building and Environment, Volume 64, 2013, pp. 46-56

APPENDIX

Table 5. Results of ultrasound test on specimen A1 by indirect method, for each of the loading steps of the compression test (Mean of three readings for each measurement between two points - Mean ultrasound velocity (m/s))

Points	**Dist.[(a)]**	**Mean ultrasound velocity (m/s)**					
	mm	**0 kN/ 0 MPa**	**50 / 1.23**	**100 / 2.47**	**200 / 4.93**	**300 / 7.40**	**400 / 9.86**
U1-U2	100	1052	1015	997	716	1113	929
U1-U3	200	1003	789	789	774	756	628
U1-U4	300	980	680	679	863	465	571
U1-U5	400	1274	548	587	377	171	-
U6-U7	100	1260	1610	1265	1606	1795	1275
U6-U8	300	754	404	628	739	641	706
U6-U9	400	755	783	630	440	510	435

Table 6. Results of ultrasound test of specimen A1 by direct method for the load steps of the compression test (Mean of three-time readings for each measurement between two points- Mean ultrasound velocity (m/s))

Points	Dist.[(a)]	**Mean ultrasound velocity (m/s)**					
	mm	**0 kN/ 0 MPa**	**50 / 1.23**	**100 / 2.47**	**200 / 4.93**	**300 / 7.40**	**400 / 9.86**
U1-U1	150	1578	1573	1562	1422	1042	890
U2-U2	150	1714	1720	1705	1684	1660	1053
U4-U4	150	1772	1771	1756	1755	1732	1754
U5-U5	150	1685	1678	1657	1620	1573	1545
U6-U6	150	1718	1728	1708	1744	1703	1743
U7-U7	150	1715	1710	1718	1718	1731	1717
U8-U8	150	1815	1797	1796	1783	1781	1772
U9-U9	150	1812	1836	1824	1821	1809	1804

Table 11. Results of ultrasound test on specimen A2 by indirect method, for each of the loading steps of the compression test (Mean of three readings for each measurement between two points - Mean ultrasound velocity (m/s))

Points	Dist.[(a)]	Mean ultrasound velocity (m/s)					
	mm	**0 kN/ 0 MPa**	**50 / 0.54**	**100 / 1.07**	**200 / 2.15**	**300 / 3.22**	**400 / 4.30**
U1-U2	100	1080	815	800	545	475	423
U1-U3	200	1095	1092	1067	874	762	570
U1-U4	300	1264	1257	1458	700	866	833
U1-U5	400	1369	1348	1620	774	1019	1040
U6-U7	100	2120	2024	2122	1081	1054	1040
U6-U8	300	2090	2091	2440	1202	1112	871
U6-U9	400	1805	1765	1774	741	573	809

Table 12. Results of ultrasound test of specimen A2 by direct method for the load steps of the compression test (Mean of three-time readings for each measurement between two points- Mean ultrasound velocity (m/s))

Points	Dist.(a)	Mean ultrasound velocity (m/s)					
	mm	**0 kN/ 0 MPa**	**50 / 0.54**	**100 / 1.07**	**200 / 2.15**	**300 / 3.22**	**400 / 4.30**
U1-U1	150	2552	2561	2613	2607	2534	2493
U2-U2	150	2588	2588	2514	2545	2551	2501
U4-U4	150	2585	2585	2488	2592	2568	2528
U5-U5	150	2552	2508	2534	2479	2560	2538
U6-U6	150	2504	2528	2510	2467	2456	2444
U7-U7	150	2493	2542	2504	2454	2436	2386
U8-U8	150	2466	2508	2501	2417	2467	2419
U9-U9	150	2552	2520	2500	2496	2466	2423

After reaching the maximum load of 490 kN (Applied vertical stress of 5.26 MPa), with the fragmentation of the base of specimen (Figure 8, Figure 9, Figure 10 and Figure 11), the test was halted and the specimen was discharged.

Table 13. Potential use of UPV testing for assessment of cracking in URM infill walls

Classification of the cracks - Crack width	Cond Par. (1) SA, SB, WTC	**Main Characteristics of cracking in URM infill walls**										**Other types of anomalies associated to cracking**		
		Vertical, horiz. or inclined crack orient. (2)	**Width of the crack** (3) Constant width (C); Variable cracks (V); Relative displacements (R) -			**Crack evolution along the time** (4) Living cracks - actives and cyclical variable or not (LC); Dead cracks- stabilised (DC)		**Crack configuration** (5) Discrete cracking: continuous/ discontinuous, linear or erratic cracks (D); Mesh/ Mapped cracking (M)		**Group of cracks of the same type**	**Crack depth**	**Spalling /peeling / exfoliation**	**Cracking in the interface between masonry and concrete elements**	**Cracking close to openings (windows doors)**
			C	**V**	**R**	**LC**	**DC**	**D**	**M**					
Negligible (0-0.1 mm)	**SB**	Mupv	Mupv	Mupv	Mupv	Mupv	Lupv	Lupv	Lupv	Lupv	Mupv	Lupv	Mupv	Mupv
	SC	Lupv	Lupv	Lupv	Lupv	Mupv	Lupv	Lupv	Lupv	Lupv	Lupv	Lupv	Mupv	Mupv
	WTC	Nupv	Nupv	Nupv	Nupv	Nupv	Nupv	Nupv	Nupv	Nupv	Nupv	Nupv	Nupv	Nupv
Thin (0.1 mm – 1 mm)	**SA**	Mupv	Mupv	Mupv	Mupv	Mupv	Lupv	Lupv	Lupv	Lupv	Mupv	Lupv	Mupv	Mupv
	SC	Lupv	Lupv	Lupv	Lupv	Mupv	Lupv	Lupv	Lupv	Lupv	Lupv	Lupv	Mupv	Mupv
	WTC	Lupv	Lupv	Lupv	Lupv	Lupv	Lupv	Lupv	Lupv	Lupv	Lupv	Lupv	Lupv	Lupv
Medium (1 mm – 3 mm)	**SA**	Mupv	Mupv	Mupv	Mupv	Lupv	Lupv	Mupv	Lupv	Lupv	Lupv	Lupv	Mupv	Lupv
	SC	Lupv	Lupv	Lupv	Lupv	Lupv	Lupv	Mupv	Lupv	Lupv	Lupv	Lupv	Lupv	Lupv
	WTC	Lupv	Lupv	Lupv	Lupv	Lupv	Lupv	Mupv	Lupv	Lupv	Lupv	Lupv	Lupv	Lupv
Large (> 3mm)	**SA**	Mupv	Mupv	Mupv	Mupv	Lupv	Lupv	Mupv	Lupv	Lupv	Lupv	Lupv	Mupv	Lupv
	SB	Nupv	Nupv	Nupv	Lupv	Nupv	Nupv	Nupv	Nupv	Nupv	Lupv	Nupv	Lupv	Lupv
	WTC	Mupv	Mupv	Mupv	Mupv	Mupv	Mupv	Mupv	Mupv	Mupv	Mupv	Mupv	Mupv	Mupv

Estimated potential interest for the use of UPV for the assessment of the state of conservation of masonry walls, aiming the definition of corrective intervention:

- Nupv - Null estimated potential interest for the use of UPV testing;
- Lupv - Low estimated potential interest for the use of UPV testing;
- Mupv - Medium estimated potential interest for the use of UPV testing;
- Hupv - High estimated potential interest for the use of UPV testing

(1) **Conditioning parameters** - **SB**: Sub-surface cracks (Internal cracking across the masonry), flaws, and voids; **SC**: Superficial cracks; **WTC**: water penetration through the cracking
(2) **Vertical, horizontal, or inclined crack orientation**
(3) **Width of the crack**: Constant width /stabilized cracks (C); variable cracks - active cracks and cyclical variable (V); Relative displacements associated to the cracks (R) - Plane displacements/ Displacements along the masonry element in depth
(4) **Crack evolution along the time**: Living cracks - actives and cyclical variable or not (LC); Dead cracks- stabilized (DC)
(5) **Crack configuration**: Discrete cracking: continuous/ discontinuous, linear or erratic cracks (D); Mesh/ Mapped cracking (M)

Contribution of Individual Authors to the Creation of a Scientific Article (Ghostwriting Policy)

José Dias had the ideas and was responsible for formulation of overarching research goals and aims of this paper; he was responsible for conducting the research and for the development of the methodology of the study; he has organized the experiments referred in the sections 4 to 9, and was responsible for their execution; he as carried out the preparation, creation of the published work.

Sources of Funding for Research Presented in a Scientific Article or Scientific Article Itself

The Planned Research Programme of the "National Laboratory of Civil Engineering" (LNEC) has funded the present study.

Conflict of Interest

The author has no conflict of interest to declare that is relevant to the content of this article.